im^2
Instituto Universitario
de Matemática Multidisciplinar

MODELLING FOR ENGINEERING & HUMAN BEHAVIOUR 2020

July 8-10, 2020

Edited by

R. Company, J.C. Cortés,
L. Jódar and E. López-Navarro

UNIVERSITAT POLITÈCNICA DE VALÈNCIA

CIUDAD POLITÉCNICA DE LA INNOVACIÓN

Modelling for Engineering & Human Behaviour 2020

València, 8 – 10 July 2020

This book includes the extended abstracts of papers presented at XXII Edition of the Mathematical Modelling Conference Series at the Institute for Multidisciplinary Mathematics "Mathematical Modelling in Engineering & Human Behaviour".

I.S.B.N.: 978-84-09-25132-2
Version: 3-12-2020
Report any problems with this document to ellona1@upvnet.upv.es.

Edited by: R. Company, J. C. Cortés, L. Jódar and E. López-Navarro.
Credits: The cover has been designed using images from kjpargeter/freepik.

This book has been supported by the European Union through the Operational Program of the [European Regional Development Fund (ERDF) / European Social Fund (ESF)] of the Valencian Community 2014-2020. [Record: GJIDI/2018/A/010].

Contents

Efficient finite element modelling of sound propagation in after-treatment devices with arbitrary cross section

F.D. Denia [♭1], E.M. Sánchez-Orgaz [♮], B. Ferrándiz [♭], J. Martínez-Casas [♭] and L. Baeza [♭]

(♭) Centro de Investigación en Ingeniería Mecánica, Universitat Politècnica de València, Camino de Vera s/n, 46022 Valencia, Spain

(♮) Instituto Univ. de Seguridad Industrial, Radiofísica y Medioambiental, Universitat Politècnica de València Camino de Vera s/n, 46022 Valencia, Spain

1 Introduction

The acoustic modelling of exhaust after-treatment devices, such as catalytic converters (CC) and diesel particulate filters (DPF) [1–3], usually requires the use of multidimensional numerical techniques to assess the influence of higher order modes on the sound attenuation performance [4]. Three-dimensional (3D) wave propagation can be considered through the finite element method (FEM). With a view to improving the computational expenditure of full 3D FEM, an efficient modelling technique is presented in this work to speed up transmission loss (TL) calculations in after-treatment devices with arbitrary cross section incorporating monoliths. The efficient modelling approach is based on the mode matching method [5–7], combining: (1) transversal pressure modes computed through a 2D FEM approach for devices with arbitrary but axially uniform cross section [8–10]; (2) compatibility conditions of the acoustic fields at the device geometric discontinuities. For the acoustic modelling of monoliths, these are replaced by four pole transfer matrices relating the acoustic fields at both sides of the monolithic region [1, 3, 4, 11–14]. Mode matching TL results are compared with full 3D FE simulations and experimental measurements for some selected configurations, showing a good agreement (results are not shown here for the sake of brevity). For a given accuracy, the computational efficiency of the mode matching technique proposed in this work improves that of full 3D FE calculations. TL improvements are achieved by suitable locations of a DPF inlet/outlet ducts. Next, a Genetic Algorithm (GA)-based optimization approach is used in order to improve the attenuation performance of the after-treatment device by varying the geometry as well as the monolith properties [15]. Results show that the optimized configuration outperforms the initial design at target frequencies [16].

Figure 1 shows the main features of the acoustic problem under consideration. Taking as reference the work presented in an earlier study [4], now the cross section of each duct/chamber is arbitrary, although axially uniform. Therefore, the transversal pressure modes are no longer available from an analytical point of view, being computed numerically in the current investigation. As indicated in the previous paragraph, a 2D FE-based numerical approach is considered

[1] e-mail: fdenia@mcm.upv.es

to solve the transversal eigenvalue problem with a view to improving the computational expenditure.

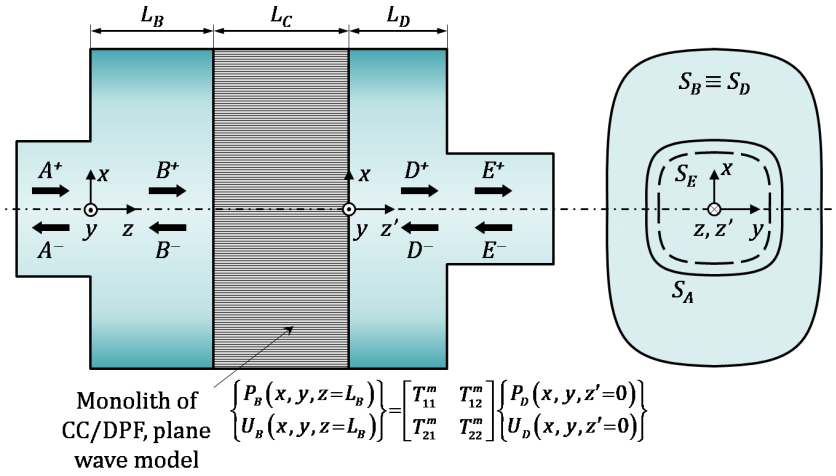

Figure 1: Exhaust after-treatment device scheme (CC/DPF) including different regions with arbitrary cross section involved in the acoustic propagation. The monolith is replaced by a transfer matrix and therefore only 1D sound propagation takes place in the capillary ducts.

In the mode matching method, the compatibility conditions of the acoustic fields (pressure and axial velocity) are expressed as weighted integrals, the weighting functions being a suitable selection of transversal pressure modes. To illustrate the approach, the pressure and velocity continuity at the inlet expansion yield

$$\int_{S_A} P_A\left(x,y,z=0\right)\psi_{A,s}\left(x,y\right)dS = \int_{S_A} P_B\left(x,y,z=0\right)\psi_{A,s}\left(x,y\right)dS \ , \tag{1}$$

$$\int_{S_A} U_A\left(x,y,z=0\right)\psi_{B,s}\left(x,y\right)dS = \int_{S_B} U_B\left(x,y,z=0\right)\psi_{B,s}\left(x,y\right)dS \ . \tag{2}$$

Expressing the acoustic fields as series expansions and taking into account the orthogonality properties of the pressure modes, the following algebraic relations are obtained:

$$\left(A_s^+ + A_s^-\right)\int_{S_A}\psi_{A,s}^2\left(x,y\right)dS = \sum_{n=1}^{N_m}\left(B_n^+ + B_n^-\right)\int_{S_A}\psi_{B,n}\left(x,y\right)\psi_{A,s}\left(x,y\right)dS \ , \tag{3}$$

$$\sum_{n=1}^{N_a} k_{A,n}\left(A_n^+ - A_n^-\right)\int_{S_A}\psi_{A,n}\left(x,y\right)\psi_{B,s}\left(x,y\right)dS = k_{B,s}\left(B_s^+ - B_s^-\right)\int_{S_A}\psi_{B,s}^2\left(x,y\right)dS \ . \tag{4}$$

Similar expressions to Eqs. (1)-(4) are obtained for the outlet contraction. Regarding the monolith, the combination of orthogonality and the plane wave transfer matrix provide

$$B_s^+\,\mathrm{e}^{-jk_{B,s}L_B} + B_s^-\,\mathrm{e}^{jk_{B,s}L_B} = T_{11}^m\left(D_s^+ + D_s^-\right) + T_{12}^m\left(k_{D,s}/\left(\rho_0\omega\right)\right)\left(D_s^+ - D_s^-\right) \ , \tag{5}$$

$$k_{B,s}/\left(\rho_0\omega\right)\left(B_s^+\,\mathrm{e}^{-jk_{B,s}L_B} - B_s^-\,\mathrm{e}^{jk_{B,s}L_B}\right) = T_{21}^m\left(D_s^+ + D_s^-\right) + T_{22}^m\left(k_{D,s}/\left(\rho_0\omega\right)\right)\left(D_s^+ - D_s^-\right) \ . \tag{6}$$

Note that, as indicated in [4], neither integrations nor modal summations appear in Eqs. (5) and (6). In addition, these equations do not depend on the geometry of the transversal cross section (provided that this is axially uniform) and relate directly wave amplitudes with

equal modal number [4].

2 Results and discussion

For illustration purposes, the approach described in the previous section is used to compute the TL-based acoustic attenuation for two DPF configurations with rectangular and triangular cross section, respectively (further details of the filter properties can be found in [2]). Rounded corners are included in both cases. Figure 2 shows information related to a number of transversal higher order modes considered in the numerical mode-matching approach.

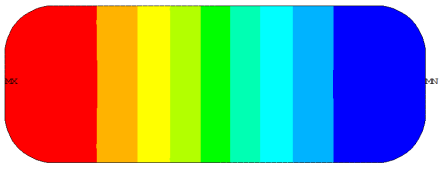

(a1): Higher order mode at 465.71 Hz.

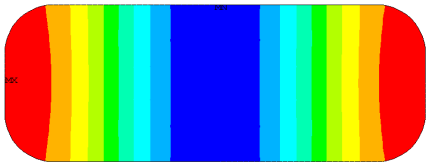

(a2): Higher order mode at 929.46 Hz.

(a)

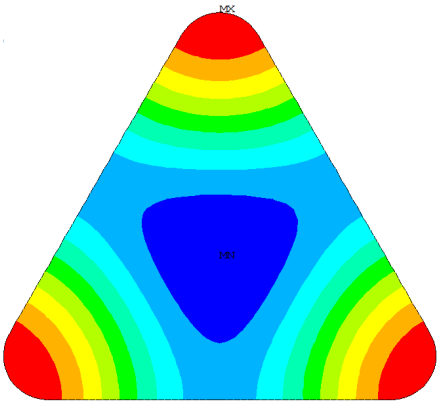

(b): Higher order mode at 1228.1 Hz.

Figure 2: Example of pressure higher order modes: (a) rounded rectangular cross section; (b) rounded triangular cross section. Green regions correspond to nodal lines (zero pressure).

As a result, the acoustic performance of the DPF is first improved following the procedure described in the literature [5], where the inlet duct is centred and the outlet is located on the nodal line of the first relevant higher order mode (see transversal modes in Fig. 2) to avoid its propagation and the corresponding detrimental effect on the TL. In the case of a circular cross section with radius R, the radial coordinate of the nodal line is $0.6276R$ [5]; for the particular rectangular cross section considered in the current investigation, the nodal line is located at a lateral distance of 0.0913 m from the centre (see mode at 929.46 Hz in Fig. 2(a)); finally, for the triangular geometry the vertical distance of the nodal line from the bottom is 0.1824 m (see mode at 1228.1 Hz in Fig. 2(b)). The beneficial impact of these duct locations on the DPF acoustic attenuation is shown in Figure 3. To outperform the initial design TL at target frequencies, a GA-based optimization approach can also be used.

With this purpose, the corresponding scheme is set up using *Matlab R2018a*, in order to perform an acoustic optimization of an after-treatment device, by obtaining the optimal chamber dimensions and monolith properties with a view to maximizing its acoustic attenuation at the frequency range $[20, 3200]$ Hz. A catalytic converter [1, 11–13] with cylindrical chamber is presented hereinafter as a case study, in order to show the validity of the proposed method. The modelling technique based on numerical mode matching, described in Section 1, is again

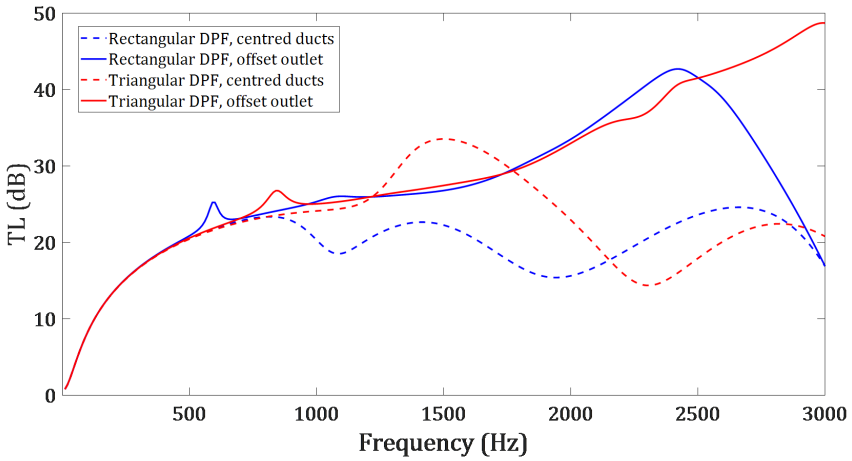

Figure 3: TL versus frequency for after-treatment devices (DPF) with rectangular and triangular cross sections. Example of attenuation improvement through outlet duct offset location.

used in order to speed up the calculation of the objective function f_0 relative to each individual during the GA optimization. f_0 is defined following [16] in order to maximize the mean TL at the target frequency range, while reducing its standard deviation to avoid steep behaviour.

Table 1 shows the range $[x_i^{min}, x_i^{max}]$ of each variable x_i involved in the GA-based optimization: lengths of the corresponding sections of the chamber L_B, L_C and L_D (see Figure 1); certain parameters of the monolith, such as resistivity R and porosity ϕ [1, 11–13]; and the position of the inlet and outlet ducts with respect to the centre of the chamber circular section: x_{in}, y_{in}, x_{out} and y_{out}.

On the other hand, attenuation increases with chamber radius R_C, and therefore this is subject to dimensional constraints. In this study, $R_C = 0.1275$ m, and so are the radii of the inlet and outlet ducts, $R_{in} = R_{out} = 0.0258$ m. Finally, the capillaries of the monolith can have a circular ◯, square □ or triangular △ cross-section.

x_i	x_i^{min}	x_i^{max}	x_i^{opt}	x_i^1	x_i^2
L_B [m]	0.05	0.15	0.0535	0.0535	0.0535
L_C [m]	0.1	0.3	0.3	0.3	0.3
L_D [m]	0.05	0.15	0.0674	0.0674	0.0674
R [rayl/m]	500	1000	1000	1000	1000
ϕ	0.7	0.9	0.9	0.9	0.9
x_{in} [m]	-0.1	0.1	-0.0778	0	0
y_{in} [m]	-0.1	0.1	0.0111	0	0
x_{out} [m]	-0.1	0.1	0.0026	-0.0778	0
y_{out} [m]	-0.1	0.1	-0.008	0.0111	0
Capillary type			△	△	△

Table 1: Range of each variable x_i.

Case $\boldsymbol{x}^{opt}$ in Table 1 shows that resistivity and monolith length values converged to the maximum values, as expected. Figure 4 shows the TL calculations for $\boldsymbol{x}^{opt}$, showing that

attenuation is maximized by offsetting the inlet duct at approximately the nodal line of the first relevant higher order mode (as described in Section 1). As expected, additional analyses show that similar attenuation is obtained by decentring the outlet duct instead of the inlet duct (case $\boldsymbol{x}^1$), while attenuation worsens when centering both ducts (case $\boldsymbol{x}^2$).

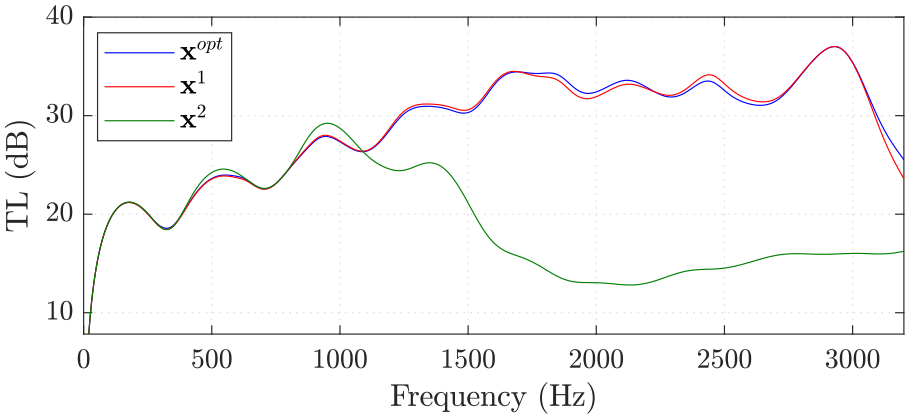

Figure 4: TL for circular cross-section CC with different inlet/outletduct configurations.

3 Conclusions and future work

An efficient modelling technique based on numerical mode matching has been presented in this work to speed up acoustic TL calculations in exhaust after-treatment devices (CC and DPF) with arbitrary cross section incorporating monoliths. The technique has been successfully combined with a GA-based optimization algorithm to obtain the optimal values of a number of design parameters (properties of the capillary ducts, type of monolith, chamber and monolith lengths, location of the inlet/outlet ducts on the chamber cross section, etc.). In future works, the effect of soot, mean flow and temperature gradients will also be studied.

Acknowledgements

The authors gratefully acknowledge the financial support of Ministerio de Ciencia, Innovación y Universidades–Agencia Estatal de Investigación through project TRA2017-84701-R and Generalitat Valenciana through project PROMETEO/2016/007.

References

[1] Selamet, A., Easwaran, V., Novak, J.M., Kach, R.A., Wave attenuation in catalytic converters: reactive versus dissipative effects. *Journal of the Acoustical Society of America*, 103: 935–943, 1998.

[2] Allam, S., Åbom, M., Sound propagation in an array of narrow porous channels with application to diesel particulate filters. *Journal of Sound and Vibration*, 291: 882–901, 2006.

[3] Jiang, C., Wu, T.W., Xu, M.B., Cheng, C.Y.R., BEM modeling of mufflers with diesel particulate filters and catalytic converters. *Noise Control Engineering Journal*, 58: 243–250, 2010.

[4] Denia, F. D., Martínez-Casas, J., Carballeira, J., Nadal, E., Fuenmayor, F. J., Computational performance of analytical methods for the acoustic modelling of automotive exhaust devices incorporating monoliths. *Journal of Computational and Applied Mathematics*, 33: 995–1006, 2018.

[5] Selamet, A., Ji, Z.L., Radavich, P.M., Acoustic attenuation performance of circular expansion chambers with offset inlet/outlet: II. Comparison with experimental and computational studies. *Journal of Sound and Vibration*, 213: 619–641, 1998.

[6] Kirby, R., Denia, F.D., Analytic mode matching for a circular dissipative silencer containing mean flow and a perforated pipe. *Journal of the Acoustical Society of America*, 122: 3471–3482, 2007.

[7] Denia, F.D., Selamet, A., Fuenmayor, F.J., Kirby, R., Acoustic attenuation performance of perforated dissipative mufflers with empty inlet/outlet extensions. *Journal of Sound and Vibration*, 302: 1000–1017, 2007.

[8] Kirby, R., A comparison between analytic and numerical methods for modelling automotive dissipative silencers with mean Flow. *Journal of Sound and Vibration*, 325: 565–582, 2009.

[9] Fang, Z., Ji, Z.L., Numerical mode matching approach for acoustic attenuation predictions of double-chamber perforated tube dissipative silencers with mean Flow. *Journal of Computational Acoustics*, 22: article number 1450004, 2014.

[10] Sánchez-Orgaz, E.M., Denia, F.D., Baeza, L., Kirby, R., Numerical mode matching for sound propagation in silencers with granular material. *Journal of Computational and Applied Mathematics*, 35: 233–246, 2019.

[11] Denia, F.D., Antebas, A.G., Kirby, R., Fuenmayor, F.J., Multidimensional acoustic modelling of catalytic converters. *16th International Congress on Sound and Vibration*, Kraków, Poland, 2009.

[12] Denia, F.D., Baeza, L., Kirby, R., Selamet, A., A multidimensional analytical study of sound attenuation in catalytic converters. *39th International Congress and Exposition on Noise Control Engineering (Inter-noise)*, Lisbon, Portugal, 2010.

[13] Denia, F.D., Martínez-Casas, J., Baeza, L., Fuenmayor, F.J., Acoustic modelling of exhaust devices with nonconforming finite element meshes and transfer matrices. *Applied Acoustics*, 73: 713–722, 2012.

[14] Sánchez-Orgaz, E.M., Denia, F.D., Martínez-Casas, J., Baeza, L., Efficient approaches for the acoustic modelling of automotive exhaust devices. Application to configurations incorporating granular materials and monoliths. *24th International Congress on Sound and Vibration*, London, UK, 2017.

[15] Fonseca de Lima, K., Lenzi, A., Barbieri, R., The study of reactive silencers by shape and parametric optimization techniques. *Applied Acoustics*, 72: 142–150, 2011.

[16] Ferrándiz, B., Denia, F.D., Martínez-Casas, J., Nadal, E., Ródenas, J.J., Topology and shape optimization of dissipative and hybrid mufflers. *Structural and Multidisciplinary Optimization*, 62: 269–284, 2020.